Quantum network theory of transport with application to the generalized Aharonov-Bohm effect in metals and semiconductors

C. H. Wu
Institute for Theoretical Physics and Synergetics, University of Stuttgart, 7000 Stuttgart 80, Federal Republic of Germany
*and Department of Electrical Engineering, University of Missouri-Rolla, Rolla, Missouri 65401**

G. Mahler
Institute for Theoretical Physics and Synergetics, University of Stuttgart, 7000 Stuttgart 80, Federal Republic of Germany
(Received 6 August 1990)

Quantum transport for resistor networks is developed with a general form factor, where each node point of the network is associated with a potential. The phase factor of the wave function in between two adjacent nodes is related to the reflection coefficient along that path. The exact transmission probability for a generalized Aharonov-Bohm ring is derived for a clean and cold crystal ring of arbitrary two-lead connections. The even- and odd-numbered rings have distinctly different transmission behaviors. The periodicity of the odd-numbered ring with respect to the threaded magnetic flux is shown to be double to that of an even-numbered one. The origin of this double periodicity is universal and is shown to be due to the standing wave produced by the two wave paths differing by odd-numbered lattice spacings at the Fermi energy. We also show that the double periodicity survives temperature averaging. Thus a mere one-atomic-spacing difference in electron paths of the ring will manifest itself in the difference of flux periodicity from the mesoscopic scale to the molecular scale.

I. INTRODUCTION

Quantum network theory has been used by a number of authors[1-6] to calculate energy spectra of a variety of molecules and solids. In this model a free electron moves on a strictly one-dimensional (1D) path joining at a node point to other one-dimensional paths. The network is generally taken in the same topology as the lattice or molecule under consideration. From such a free-electron network, Coulson[2] has calculated the density of states for graphite. Ruedenberg and Scherr[3] have shown that, as a consequence of momentum conservation, a Kirchhoff law has to be satisfied at each node point. Della Riccia[4] has used the free-electron network for investigation of diamond. Weger *et al.*[5] used the free-electron network with directed bonds to study anomalously high peaks of the density of states in the β-W structure. Montroll has generalized the free-electron network to incorporate a periodic potential associated with the 1D path[6] and to calculate the surface density of states from such a model.[7] One of us has extended Montroll's model to investigate interface states and superlattice electronic states.[8] A semiconductor or diatomic network has also been studied.[9] In either a free-electron network or a network associated with a periodic potential, the density of states is obtained by imposing a Bloch condition when a unit cell is translated to the next in a crystalline structure. Surface or local disorder can then be considered as an additional perturbation.

In recent years, the wave motion of electrons in quasi-one-dimensional mesoscopic structures has been extensively studied.[10-19] This is not only due to the advances in lithographic techniques available for fabricating such structures but also due to the strong drive of using the wave nature of electrons for the next generation electronic devices.[15,20] The quasi-one-dimensional electron wave motion exists not only in metals, such as the Aharonov-Bohm-type conducting rings, but also in GaAs devices, where ballistic transport has been shown to be possible[21] and where the edge channels can be viewed as independent 1D current channels.[22] Thus quasi-one-dimensional electron networks become widely available on mesoscopic scale in addition to superconducting networks. Such a mesoscopic theory of electron transport is characterized by the wave motion of electrons in a total system size of M atoms, where M is large but is not allowed to take the $M \rightarrow \infty$ limit and all length ratios in the structure remain rational numbers. The quantum transport theory is based on the Landauer-Buttiker formalism,[10-12,23,24] where the conductance between two points is determined by the transmission probability from one point to the other. The disorder of the material as well as the structure between the two points determine such a transmission probability.

The treatment of such spatially inhomogeneous structures favors the use of local schemes, such as tight-binding or quantum-network models. Both are semiempirical in that they require parameters in terms of matrix elements or "bond" potentials, respectively, on a topological net, and both are designed to make efficient use

of given bulk material properties. The underlying picture, however, is quite different. The network model is defined by a local rule resulting from boundary conditions, the so-called node equation, which may vary from node to node to account for local parameter variations and different connectivities. This node equation is determined by the use of a Kirchhoff law at a given node and there is a formal analogy with classical resistor-network theory. On a microscopic level the net constitutes the atomic structure, and the wave equation is the single-electron Schrödinger equation with an appropriate atomic potential, which determines the form factor entering the node equation. This allows one to simulate any bulk dispersion relation, not just tight-binding results. We note in passing that on a mesoscopic level the net may be related to a superstructure (e.g., superlattice), and the wave equation could be the effective-mass Schrödinger equation with varying band edge. Along these lines a free-electron-like node equation has been investigated by Doucot and Rammal[25] for normal-metal networks from the Cooperon equation in the weak-localization regime. DeGennes[26] and Alexander[27] have derived a free-electron-like node equation from the Landau-Ginzburg equation for superconducting networks.

It is with this advantage for more complicated 1D networks in mind that we try to develop here the quantum network theory of transport for clean metals and semiconductors. However, in the transport theory, there is a major deviation from the traditional quantum-network theory. When only eigenenergies are to be determined, the electron wave is allowed to travel in one direction and hence a Bloch condition can be imposed when one moves from one unit cell to the next. In transport theory, there exist both transmitted and reflected waves on the 1D path, therefore the Bloch theorem does not apply and one has to take care of the phase factor in the wave function properly. This is described in Sec. II for a free-electron network (Sec. II A) as well as for a network with each node point associated with a potential (Sec. II B). The form factor derived for a one-band metallic model allows a generalization to more realistic materials as well as for the quasi-one-dimensional (multichannel) case by means of simple substitution of this factor. The form factor for a two-band model that is suitable for describing semiconductors is given in Sec. II C. The Kirchhoff law used here might be generalized to include different strengths to different inequivalent bonds and hence different couplings between the connecting leads and the ring with additional adjustable parameters.[2,5,28]

We apply the theory to a clean and cold generalized Aharonov-Bohm-type ring with two connecting leads and derive the general and exact transmission probability for such a ring of an arbitrary form factor. This is given in Sec. III with the use of a complex Green's function that is suitable for extension to include a small amount of disorder in the ring. In the case of an exact symmetric ring, our quantum-network theory of transport agrees with the result of Buttiker-Imry-Azbel[11] and the result corresponds to their case of some strong coupling between the connecting leads and the ring. The transmission probability at the Fermi level for a ring with an even number of atoms is periodic in the magnetic flux Φ with period $\Phi_0=hc/e$, where Φ_0 is the normal flux quantum, regardless of the two connecting locations. However, at certain locations, good resemblance of double periodicity, $\Phi_0/2$, will emerge. The result for an odd-numbered ring is quite different and is shown to have double periodicity regardless of the connecting locations. In particular, when the ring is large and the two paths differ by just one atomic spacing, our result should have important implications. This is discussed in Secs. IV and V along with calculations of transmission probabilities as function of energy and magnetic flux in metal and semiconductor rings. We also evaluate the behavior of transmission probability at finite temperature and show that double periodicity is not destroyed. Our conclusions are given in Sec. VI.

II. NODE EQUATION FOR QUANTUM TRANSPORT

A quantum network is generally constructed to be topologically equivalent to that of the crystal, the mesoscopic structure or molecule of interest. For example, a generalized Aharonov-Bohm-type ring of radius r_0 is shown in Fig. 1(a). Here, we assume that the width of the wire is small relative to all other length scales of the problem,[28] so that an idealization of the physical structure can be made. Each of the M node points is at the center location of an atom, which is held fixed, and is connected to neighboring node points by 1D bonds. The number of such bonds for a given node defines its coordination numbers, which for the present topology varies between 2 and 3. The lattice spacing is $l=2\pi r_0/M$. In the segment between any two nodes, there exists a 1D wave function that satisfies the Schrödinger equation. Three cases of 1D bonds are considered.

A. Node equation for free-electron model

Let us take a segment between m_0 and m_1 node points as shown in Fig. 1(a) with $x=0$ at node m_0 and $x=l$ at node m_1. The solution of the wave function $\psi_{m_0m_1}(x)$ from the Schrödinger equation can be written as a superposition of two plane waves from the two directions. Thus

$$\psi_{m_0m_1}(x)=e^{-iS_{m_0m_1}(x)/\hbar}(A_{m_0m_1}e^{ikx}+B_{m_0m_1}e^{-ikx}) =e^{-iS_{m_0m_1}(x)/\hbar}a_{m_0m_1}\cos(kx+\delta_{m_0m_1}) , \quad (1)$$

where

$$a_{m_0m_1}=4A_{m_0m_1}B_{m_0m_1} \quad (2)$$

is the complex amplitude, and

$$\tan\delta_{m_0m_1}=-i\left[\frac{A_{m_0m_1}-B_{m_0m_1}}{A_{m_0m_1}+B_{m_0m_1}}\right] =-i\left[\frac{1-R_{m_0m_1}}{1+R_{m_0m_1}}\right] , \quad (3)$$

where $\delta_{m_0m_1}$ is the complex phase factor and $E=\hbar^2k^2/2\mu$.

The function $R_{m_0m_1}=B_{m_0m_1}/A_{m_0m_1}$ is the reflection coefficient facing toward the m_0 node. If a tangential vector potential $\mathbf{A}(x)$ is also present, an electron moving from the m_0 node toward the m_1 node will accumulate an additional phase shift $S_{m_0m_1}(x)$, which is given by

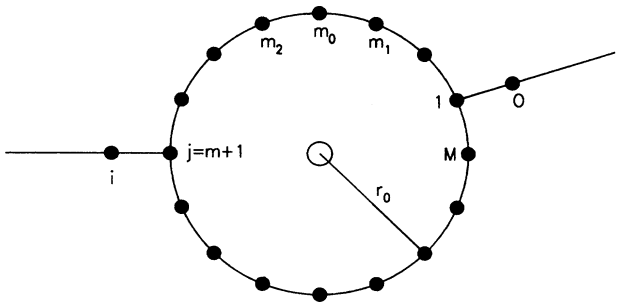

(a)

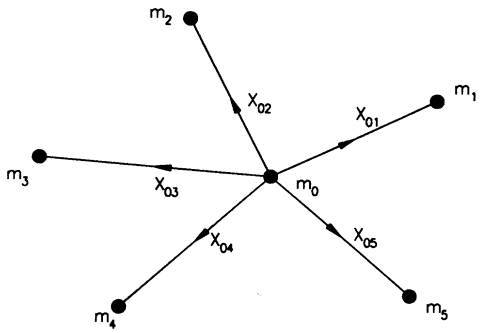

(b)

FIG. 1. (a) A generalized Aharonov-Bohm ring with one input lead and one output lead. The system is made of the same material and each node point is centered at an atom. An electron from the input node i will sample m nodes clockwise and n nodes counterclockwise to arrive at the output node o. The magnetic flux Φ is threaded at the center (open circle) of the ring of radius r_0, where the total number of atoms is $M=m+n$ and the lattice spacing between two atoms is l. The numbering of nodes is from the output node counterclockwise. (b) A general case of a node point m_0 connecting to several other node points, where Kirchhoff's law at m_0 is given by Eq. (7) with summation α running over all segments. Here, $x=0$ is located at the m_0 node with the positive coordinate $x_{o\alpha}$ toward the m_α node.

$$S_{m_0m_1}(x)/\hbar=\frac{e}{\hbar c}\int_{m_0}^{x}\mathbf{A}(x')\cdot d\mathbf{x}'=\frac{x}{r_0}\left[\frac{\Phi}{\Phi_0}\right]. \quad (4)$$

We note that in the earlier quantum-network calculations, only the eigenenergy is sought after, the electron is then allowed to move in one direction. In this case, $\tan\delta_{m_0m_1}=\pm i$ for each direction. However, in quantum transport, both transmitted and reflected waves are present, the general complex phase factor is related to the reflection coefficient by Eq. (3). Thus if we denote the wave function at node m_0 as $\psi_{m_0m_1}(m_0)=a_{m_0m_1}\cos\delta_{m_0m_1}$, the wave function at m_1 is

$$\psi_{m_0m_1}(m_1)=\psi_{m_0m_1}(m_0)e^{-iS_{m_0m_1}(l)/\hbar}\times(\cos kl-\tan\delta_{m_0m_1}\sin kl)\ . \quad (5)$$

If the m_0 node is connected to the m_1 and m_2 nodes only as in Fig. 1(a), then there are two segments joining at the node and the conditions at the m_0 node require that the wave functions and their respective derivatives be equal. The second condition is the statement of conservation of momentum or Kirchhoff's law, which can be generalized to include scattering at the node point and different cross sections of the respective channels so that[2,27,28]

$$\sum_\alpha \nu_{m_0m_\alpha}\frac{\partial\psi_{m_0m_\alpha}(x)}{\partial x}\bigg|_{m_0}=\eta_{m_0}\psi(m_0)\ , \quad (6)$$

where α runs over all segments joining at node m_0 [see Fig. 1(b)]. η_{m_0} is the parameter representing a δ-function potential, and the $\nu_{m_0m_1}$ parameter allows one to provide different coupling strengths. We will settle for an exact momentum conservation in equal cross sections of all bond segments. Thus $\eta_{m_0}=0$ and $\nu_{m_0m_1}=1$ leading to the condition

$$\sum_\alpha\frac{\psi'_{m_0m_\alpha}(m_0)}{\psi_{m_0m_\alpha}(m_0)}=\sum_\alpha\left[\frac{-i}{\hbar}\frac{dS_{m_0m_\alpha}}{dx}\bigg|_{m_0}-k\tan\delta_{m_0m_\alpha}\right]=0\ , \quad (7)$$

for any m_0, where

$$\psi'_{m_0m_\alpha}(m_0)=\frac{d\psi_{m_0m_\alpha}(x)}{dx}\bigg|_{x=0}\ .$$

In the case of Fig. 1(a), Eq. (7) is reduced to

$$\sum_{\alpha=1}^{2}\tan\delta_{m_0m_\alpha}=0\ , \quad (7a)$$

because the two derivatives of phase factors originating from the magnetic flux cancel each other. A similar equation for Eq. (5) can be obtained between nodes m_0 and m_2 so that when Kirchhoff's law of Eq. (7a) applies, we have, for any m_0

$$2\cos kl\,\psi(m_0)-e^{-i\theta}\psi(m_2)-e^{i\theta}\psi(m_1)=0\ , \quad (8)$$

where the form factor for free electron is $F(E)=\cos(kl)$

and $\theta=(l/r_0)(\Phi/\Phi_0)$. The node equation for higher coordination numbers can be written similarly.

B. Node equation for a single-band model

It is very important to establish a node equation where there is a potential associated with each node point. This has been developed by Montroll.[7] While there are a few simple potentials, such as a step potential well, that can provide an easy solution for the wave function along the segment, a potential well of $V(x)$ such that

$$\frac{2\mu V(x)}{\hbar^2}=-2\gamma^2\mathrm{sech}^2\gamma x \tag{9}$$

has been found to be more useful.[7] Here μ is the electron mass and γ is a parameter. We will model our calculations based on this potential to illustrate a general result. The potential is shown in Fig. 2. The solution of the Schrödinger equation along the segment between m_0 and m_1 is then

$$\psi_{m_0m_1}(x)=a_{m_0m_1}\left[\cos(kx+\delta_{m_0m_1})-\frac{\gamma}{k}\sin(kx+\delta_{m_0m_1})\tanh\gamma x\right], \tag{10}$$

where $a_{m_0m_1}$ and $\delta_{m_0m_1}$ are two complex constants of integration as in the free-electron case, and $E=\hbar^2k^2/2\mu$. The solution of Eq. (10) provides one bound state in a one-atom ring. In quantum transport, Eq. (3) for the phase factor $\delta_{m_0m_1}$ is modified to

$$\tan\delta_{m_0m_1}=\pm i\left[\frac{\sqrt{1-F^2}}{D}\right]\left[\frac{R_{m_0m_1}-1}{R_{m_0m_1}+1}\right] \tag{11}$$

and Eq. (5) to

$$\psi_{m_0m_1}(m_1)=e^{-i\theta}\psi_{m_0m_1}(m_0)(F-D\tan\delta_{m_0m_1}), \tag{12}$$

where

$$D=\frac{2s(c+u)}{1+cu+sv} \tag{13}$$

and

$$s=\sin\left[\frac{kl}{2}+\xi\right], \tag{14a}$$

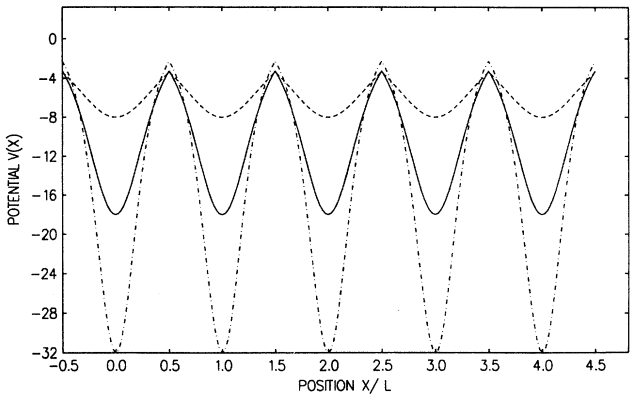

FIG. 2. Periodic potential for a 1D chain using the potential $V(x)$ given by Eq. (9). The atoms are centered at $x/l=0,1,2,3,4$ sites and $\gamma l=2$ (dotted curve), $\gamma l=3$ (solid curve), and $\gamma l=4$ (dash-dotted curve).

$$c=\cos\left[\frac{kl}{2}+\xi\right], \tag{14b}$$

$$u=\left[\frac{\gamma}{k}\right]^2\cos\xi\,\mathrm{sech}^2\frac{\gamma l}{2}\cos\frac{kl}{2}, \tag{14c}$$

$$v=\left[\frac{\gamma}{k}\right]^2\cos\xi\,\mathrm{sech}^2\frac{\gamma l}{2}\sin\frac{kl}{2}, \tag{14d}$$

with

$$\tan\xi=\left[\frac{\gamma}{k}\right]\tanh\frac{\gamma l}{2}. \tag{14e}$$

Kirchhoff's law of Eq. (7) remains true except that k is replaced by $[1+(\gamma/k)^2]$. Thus for a closed ring of M atoms with magnetic flux threaded in the center as in Fig. 1(a), Eq. (7a) applies and the node equation can be written as

$$2F(E)\psi(m)-e^{-i\theta}\psi(m+1)-e^{i\theta}\psi(m-1)=0, \tag{15}$$

where $m=1,2,3,\ldots,M$ and the form factor $F(E)$ is given by

$$F(E)=\left[1+\left[\frac{\gamma}{k}\right]^2\right]^{-1}\left\{\left[1+\left[\frac{\gamma}{k}\right]^2\left[1-2\tanh^2\frac{\gamma l}{2}\right]\right]\cos kl-\left[\frac{\gamma}{k}\right]\left[2+\left[\frac{\gamma}{k}\right]^2\mathrm{sech}^2\frac{\gamma l}{2}\right]\sin kl\tanh\frac{\gamma l}{2}\right\}. \tag{16}$$

In deriving Eq. (16), all node points are taken to be identical and potentials are joining at the midpoints between the adjacent nodes. The eigenenergies E satisfy

$$F(E_S)=\cos\frac{2\pi}{M}\left[S\mp\frac{\Phi}{\Phi_0}\right] \tag{17}$$

with the corresponding wave function $\psi(m)$ given by

$$\psi(m)=\psi_0e^{\pm 2\pi iS(m/M)}, \tag{18}$$

where the $\pm$ sign denotes the counterclockwise and clockwise directions of propagation and $S=1,2,3,\ldots,M$. The ordering of eigenenergies E_S with

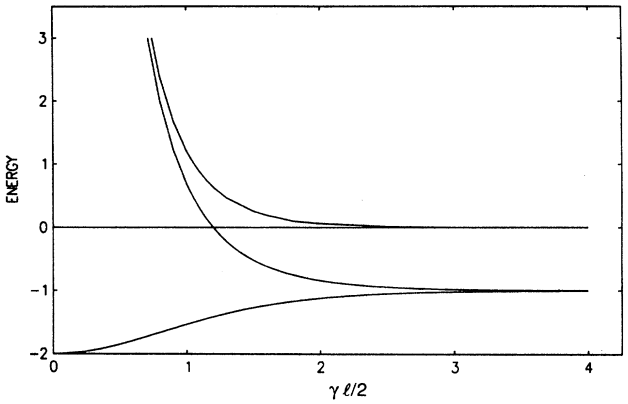

FIG. 3. Energy band E (in units of $\hbar^2\gamma^2/\mu$) as a function of $\gamma l/2$, where $-\hbar^2\gamma^2/\mu$ is the depth of the potential well and l is the lattice spacing. The band edges are determined by the condition that $|F|\leq 1$. At $\gamma l/2=4.0$, a very narrow band exists in the negative energy range, where $E=-2.0$ is the bottom of the potential well, and continuum states start at $E=0$. At $\gamma l/2=1.5$, the energy band ranges from $E=-1.27$ to -0.51 and continuum states start at $E=+0.26$. For $\gamma l/2=0$, the free- electron limit is reached.

respect to the quantum number S from the lowest energy upward can be determined by Eq. (17). For example, if $M=8$, the ordering is $S=8,1,7,2,6,3,5,4$ for $\Phi>0$ and $S=8,7,1,6,2,5,3,4$ if $\Phi<0$. In the case of the 1D ring with no magnetic flux, the band structure is shown in Fig. 3 as a function of the dimensionless parameter $\gamma l/2$, where the potential well depth is $\hbar^2\gamma^2/\mu$ and l is the lattice spacing. The bound-state solution can be obtained by replacing k with ik. (We note that any exact solution

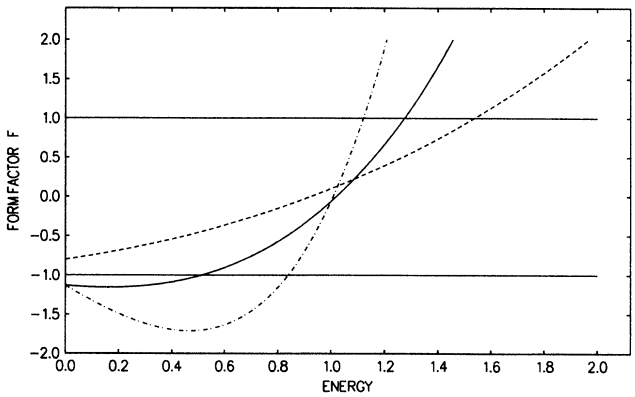

FIG. 4. Form factor $F(E)$ as function of energy E (in units of $\hbar^2\gamma^2/\mu$) in the bound-state region. Shown here is $\gamma l/2=1.0$ (dashed curve), $\gamma l/2=1.5$ (solid curve), and $\gamma l/2=2.0$ (dash-dotted curve). When $\gamma l/2$ is small, $F(E)$ is closer to a cosine-like function in the allowed energy range determined by $|F|\leq 1.0$ and a free-electron energy-momentum relation is reached. When $\gamma l/2$ is large, $F(E)$ is closer to a linear relation of E and the tight-binding limit is reached.

of the 1D crystal chain with a periodic potential must have a solution of the form of Eq. (17). When $\gamma l/2$ is large, the tight-binding limit is obtained because $F(E)\sim c_1+c_2E$. On the other hand, in the free-electron limit, $F(E)\sim\cos[(\sqrt{2\mu E}/h)l]$.) Thus, if we express E_S in a Fourier series, one can rewrite Eq. (17) equivalently as

$$E_S=\sum_{n=0}^{\infty}a_n\cos\frac{2\pi n}{M}\left[S\mp\frac{\Phi}{\Phi_0}\right], \tag{19}$$

so that we can see that whenever Eq. (17) is used, all higher harmonics of S and Φ/Φ_0 are included.

We note that any realistic 1D band-structure calculation can always be rearranged into the form of Eq. (17) so that a realistic form factor is assured. Equation (17) is also a result of the Korriga-Kohn-Rostoker method of a band-structure calculation where lattice structure and periodic potential are segregated on each side of the equation.[29] This will allow one to realize multichannel or quasi-one-dimensional results more quickly. The form factor $F(E)$ from Eq. (16) is plotted as a function of dimensionless energy $E(\mu/\hbar^2\gamma^2)$ in Fig. 4, for various values of $\gamma l/2$, in the bound-state region in which we are interested.

C. Node equation for a semiconductor model

To model a 1D semiconductor network, the associated potential at each node should have two more bound states in a closed ring. This could be achieved by generalizing the potential $V(x)$ in Eq. (9) into

$$V(x)=-V_0\mathrm{sech}^2\gamma x\ . \tag{20}$$

However, the solution is then inconveniently expressed in terms of hypergeometric functions.[30] An alternative and simpler way is to form a unit cell with two different atoms corresponding to two different potential-well depths. This will allow one to express the wave function in circular and hyperbolic functions. In a diatomic ring of alternating potential-well depths of γ_0 and γ_1, node m_0 of γ_0 is joining at $x=l_0$ with node m_1 of γ_1 at $x=-l_1$ so that the total spacing between the two nodes is $l=l_0+l_1$. Thus, for the m_0 node, the equivalent Eq. (5) is

$$e^{-i\theta}\psi_{m_0m_1}(m_0)(F_0-D_0\tan\delta_{m_0m_1})=\psi_{m_0m_1}(m_1) \tag{21}$$

and similarly for the adjacent m_1 node,

$$e^{i\theta}\psi_{m_1m_0}(m_1)(F_1-D_1\tan\delta_{m_1m_0})=\psi_{m_1m_0}(m_0)\ , \tag{22}$$

where

$$F_0=\frac{c_0(c_1+u_1)-(s_0+v_0)s_1}{c_1^2+s_1^2+c_1u_1+s_1v_1} \tag{23}$$

and

$$D_0=\frac{s_0(c_1+u_1)+(c_0+u_0)s_1}{c_1^2+s_1^2+c_1u_1+s_1v_1}\ , \tag{24}$$

with

$$c_0=\cos kl_0-\frac{\gamma_0}{k}\sin kl_0\tanh\gamma_0 l_0 \ , \tag{25a}$$

$$s_0=\sin kl_0+\frac{\gamma_0}{k}\cos kl_0\tanh\gamma_0 l_0 \ , \tag{25b}$$

$$u_0=\left[\frac{\gamma_0}{k}\right]^2\operatorname{sech}^2\gamma_0 l_0\cos kl_0 \ , \tag{25c}$$

$$v_0=\left[\frac{\gamma_0}{k}\right]^2\operatorname{sech}^2\gamma_0 l_0\sin kl_0 \ , \tag{25d}$$

and

$$\tan\delta_{m_0m_1}=\pm\frac{i\sqrt{1-F_0F_1}}{D_0}\frac{R_{m_0m_1}-1}{R_{m_0m_1}+1} \ . \tag{25e}$$

Similarly c_1, s_1, u_1, and v_1, are obtained by replacing γ_0 and l_0 with γ_1 and l_1. D_1 and F_1 are obtained by interchanging the two indices in Eqs. (24) and (25). Since Kirchhoff's law of Eq. (7a) remains valid at each node point, the net effect of having two atoms per unit cell is to replace the monatomic form factor by diatomic form factor, which can be written as

$$F(E)=(F_0F_1)^{1/2} \ . \tag{26}$$

In addition to the condition that $|F(E)|\leq 1$, the band gap between valence band and conduction band appears at the energy at which F_0 (F_1) is positive while F_1 (F_0) is negative. An example of the energy gap for a diatomic ring is illustrated in Fig. 5. Thus, with a mere substitution by the diatomic form factor, the node equation for the semiconductor network can be obtained, using the corresponding Eq. (11) for the phase relation of the wave function in the diatomic case, which is given in Eq. (25e).

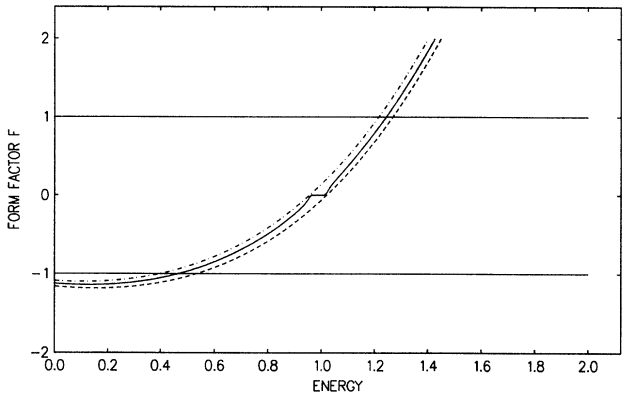

FIG. 5. Diatomic form factor $F=(F_0F_1)^{1/2}$ for modeling semiconductor networks. The additional energy gap is determined by the condition when the product F_0F_1 is negative. Here $\gamma_0 l_0/2=1.5$ for F_0 (dashed curve) and $\gamma_1 l_1/2=1.45$ for F_1 (dash-dotted curve) and F (solid curve) has two branches, connected by a solid bar at $F=0$ to indicate the band gap. Energy E is in units of $\hbar^2\gamma_0^2/\mu$ and $l_0=l_1=l/2$ is used. When the difference between γ_0 and γ_1 is increased, the band gap increases.

III. QUANTUM TRANSPORT THROUGH A GENERALIZED AHARONOV-BOHM RING

In the Landauer-Buttiker formalism, the conductance between two points, say between i and o, depends on the transmission probability from point i to point o. Referring to Fig. 1(a), a generalized Aharonov-Bohm ring of $M=m+n$ atoms is composed of two paths, so that from point i clockwise, one encounters m atoms (or m nodes) in the ring while counterclockwise, n atoms. The asymmetry is given by $\Delta=|m-n|$. If we consider such a ring as an obstacle box between the two connecting leads, then the transmission probability from point i to point o at zero temperature will generally depend on the energy of an incoming electron wave and the magnitude of magnetic flux even though the ring has a perfect crystalline structure. The two connecting leads can be considered as a perturbation to a closed ring so that at an arbitrary node point j, the wave function at the node point $\psi(j)$ satisfies a matrix equation that can be written as

$$2F\psi(j)-e^{-i\theta}\psi(j+1)-e^{i\theta}\psi(j-1)=G(j) \ , \tag{27}$$

where $j=1,2,3,\ldots,M$ and

$$G(j)=\delta_{j,1}[\psi_0-F\psi(1)]+\delta_{j,m+1}[\psi_i-F\psi(m+1)] \ . \tag{28}$$

An electron moving along the connecting leads will not accumulate an additional phase factor due to the magnetic flux. ψ_0 and ψ_i are wave functions at one lattice spacing from the ring at each connecting lead. From Eq. (12), we have

$$\psi_i=\left[F\pm i\sqrt{1-F^2}\left[\frac{R-1}{R+1}\right]\right]\psi(m+1) \tag{29}$$

and

$$\psi_0=(F+i\sqrt{1-F^2})\psi(1) \ . \tag{30}$$

Here, a Bloch condition is imposed between node 1 and node 0 in Eq. (30), since only an outgoing wave exists, while, between node $m+1$ and node i, the general relation of phase factor from Eq. (11) applies. $F(E)$ is the general form factor whose expressions for metallic and semiconductor models has been described in Sec. II. The solution of Eq. (27) can be obtained by introducing a complex Green's function $g(j)$ that satisfies

$$2Fg(j)-e^{i\theta}g(j-1)-e^{-i\theta}g(j+1)=\delta_{j,M} \ . \tag{31}$$

$g(j)$ has a solution that can be written as

$$g(j)=\frac{1}{2M}\sum_{S=1}^{M}\frac{e^{\pm 2\pi iSj/M}}{F-\cos\frac{2\pi}{M}\left[S\mp\frac{\Phi}{\Phi_0}\right]} \ . \tag{32}$$

Note that $g(j)$ is the exact 1D Green's function and is not a tight-binding Green's function, because $F(E)$ is in general not linear in energy as mentioned earlier. The upper (lower) sign is for the counterclockwise (clockwise) direction of propagation and $g(-j)=g^*(j)$. By substituting Eq. (28) into Eq. (27) and setting $j=1$ and $m+1$, respectively, we have two homogeneous equations for $\psi(1)$ and $\psi(m+1)$. After solving for the reflection coefficient R from the secular determinant, we have

$$R=\frac{(1-F^2)[|g(m)|^2-g^2(0)]-1}{(1-F^2)[|g(m)|^2-g^2(0)]+1-i2\sqrt{1-F^2}g(0)} . \tag{33}$$

Here $g(0)$ is a real quantity. The "in-band" complex Green's function ($|F|\leq 1$) can be summed in closed form so that the transmission probability $T=1-|R|^2$ can be written as

$$T=\frac{4\left[\sin^2 m\beta+\sin^2 n\beta+2\sin m\beta\sin n\beta\cos\frac{2\pi\Phi}{\Phi_0}\right]}{4\left[\sin^2 m\beta+\sin^2 n\beta+2\sin m\beta\sin n\beta\cos\frac{2\pi\Phi}{\Phi_0}\right]+\left[\sin m\beta\sin n\beta-2\left[\cos\frac{2\pi\Phi}{\Phi_0}-\cos M\beta\right]\right]^2} , \tag{34}$$

where

$$\cos\beta=F(E) . \tag{35}$$

We note that the Green's function of Eq. (32) also has "out-of-band" solutions, corresponding to regions with $|F|>1$. However, if the ring and the connecting leads are considered as being made of the same materials, no incoming wave with out-of-band energy can be prepared. The situation would be different if different materials were used. In that case, Eq. (28) had to be modified and out-of-band solutions would contribute to the transmission probability.

Equation (34) provides the exact expression of transmission probability of the generalized Aharonov-Bohm ring with an arbitrary form factor and is symmetric with respect to the interchange of m and n. The use of different form factors (hence different periodic potentials) differs in the mapping of this factor into the energy space only.

In the special case of a symmetric ring, M is an even number and $m=n=M/2$, so that Eq. (34) is reduced to

$$T=\frac{4\left[\sin\frac{M\beta}{2}\cos\frac{\pi\Phi}{\Phi_0}\right]^2}{\left[-\frac{5}{4}\cos M\beta+\cos\frac{\pi\Phi}{\Phi_0}+\frac{1}{4}\right]^2+\sin^2 M\beta} . \tag{36}$$

By comparing Eq. (36) with Buttiker-Imry-Azbel's result [Eq. (4.25) of Ref. 11], it is clear that our quantum-network result corresponds to the use of an S matrix of the form

$$S=\begin{bmatrix} \frac{1}{3} & \frac{2}{3} & \frac{2}{3} \\ \frac{2}{3} & -\frac{1}{3} & \frac{2}{3} \\ \frac{2}{3} & \frac{2}{3} & -\frac{1}{3} \end{bmatrix} , \tag{37}$$

which represents a case of strong coupling between the connecting leads and the ring (that is $\epsilon=\frac{4}{9}$ close to the maximum value of $\epsilon=\frac{1}{2}$ in Ref. 11). As mentioned earlier, a different coupling can be accomplished by introducing additional parameters in Kirchhoff's law as shown in Eq. (6). Our result relies on a strict conservation of momentum with equal cross sections for connecting all bonds. Finally, in the extreme case where the two connecting leads are merged into one, only the second term of Eq. (28) exists and $R=-e^{-i\varphi}$, where the accumulated phase φ can be written as

$$\varphi=2\tan^{-1}\left[\frac{1}{2}\frac{\sin M\beta}{\cos\left[\frac{2\pi\Phi}{\Phi_0}\right]-\cos M\beta}\right] . \tag{38}$$

IV. AHARONOV-BOHM OSCILLATIONS

The periodicity of the transmission probability at an incident electron energy corresponding to the highest occupied state at zero temperature (and hence called the Fermi energy, E_F, here) has been studied by many authors.[10–19,31,32] This periodicity depends on whether the number of atoms on the ring is even or odd. When M is even, there are two classes of even numbers: E_F is located at $M/4$ for $\Phi>0$ and at $3M/4$ for $\Phi<0$ if $M=(4,8,12,16,\ldots,4N,\ldots,)$. Similarly, E_F is located at $(3M+2)/4$ for $\Phi>0$ and at $(M-2)/4$ for $\Phi<0$, if $M=(2,6,10,14,\ldots,4N+2,\ldots,)$. Note that Eq. (34) is symmetric with respect to Φ. When M is an even number of either class and $m=M/2$, Eqs. (34) or (36) indicate a periodicity of Φ_0. When M is an odd number, there are again two classes: E_F is located at $(3M+1)/4$ for $\Phi>0$ and located at $(M-1)/4$ for $\Phi<0$, if $M=(1,5,9,\ldots,4N+1,\ldots,)$. Similarly, E_F is located at $(M+1)/4$ for $\Phi>0$ and located at $(3M-1)/4$ for $\Phi<0$, if $M=(3,7,11,\ldots,4N+3,\ldots,)$. In either case, the periodicity is exactly doubled. This can be shown, for example, by observing the $4N+1$ type of odd numbers. Substituting the values of E_F into Eq. (35), we have

$$F(E_F,\Phi>0)=\sin\frac{2\pi}{M}(\tfrac{1}{4}-\Phi/\Phi_0) \tag{39}$$

and

$$F(E_F,\Phi<0)=\sin\frac{2\pi}{M}(\tfrac{1}{4}+\Phi/\Phi_0) . \tag{40}$$

Thus, in addition to T being symmetric with respect to the origin of Φ, Eqs. (39) and (40) provide that

$$F(E_F,\Phi/\Phi_0=-0.5+x)=-F(E_F,\Phi/\Phi_0=x) \tag{41}$$

for $0\leq x\leq 0.5$. Referring to Eq. (35), this leads to

$$\sin m\beta_+=+\sin m\beta_- , \tag{42}$$

$$\sin n\beta_+=-\sin n\beta_- , \tag{43}$$

and

$$\cos\left[\frac{2\pi\Phi}{\Phi_0}\right]\Bigg|_{-0.5+x} = -\cos\left[\frac{2\pi\Phi}{\Phi_0}\right]\Bigg|_{x}, \tag{44}$$

where m is odd and n is even [change signs in Eqs. (42) and (43) if m is even and n is odd] and β_+ (β_-) is positive (negative). Therefore, both the numerator and denominator of Eq. (34) are unchanged so that

$$T\left[\frac{\Phi}{\Phi_0}=-0.5+x\right]=T\left[\frac{\Phi}{\Phi_0}=x\right]. \tag{45}$$

We note that this double periodicity is exact for any combination of (m,n) pairs and M values, regardless of the choice of the form factor. It is thus a universal double periodicity.

In particular, we are interested in the case of the closest possible configuration of a symmetric ring. Experimentally, the Aharonov-Bohm effect has been measured and the existence of both single and double periodicity in a mesoscopic sample has been established.[14] The $\Phi_0/2$ periodicity has been attributed to various sources by other authors.[11,18,19,31,32] In disordered materials, the $\Phi_0/2$ period of transport has been related to the interference of conjugated waves. The effects due to impurity scattering, temperature, and electron-electron interaction have been reported.[18,19,31,32] However, here we show that even in a clean crystal ring of odd-numbered atoms at zero temperature, double periodicity in transmission probability is exact at any connecting configuration. Incident electrons at the Fermi energy of an odd-numbered ring will arrive at the output node with totally cancelled amplitudes and the resultant standing wave along the input lead and the ring is similar to the backscattering interference[33] for a disordered ring that produces the double periodicity. However, our standing wave is produced by a fixed geometry on a crystalline ring. This additional possibility for the origin of double periodicity can be applied to Aharonov-Bohm effect on a mesoscopic scale as well as on a molecular scale. In a thick disordered ring,

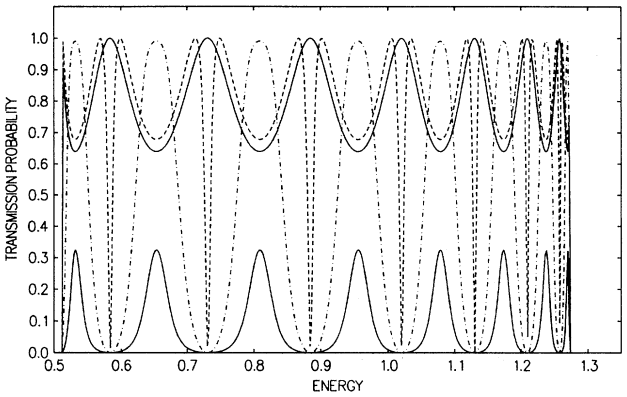

FIG. 6. Transmission probability $T(E)$ as function of energy E, in units of $\hbar^2\gamma^2/\mu$, in the energy band of one-band metallic model with $\gamma l/2=1.5$. Here Φ/Φ_0 are 0 (upper solid curve), 0.1 (dashed curved), 0.35 (dash-dotted curved), and 0.45 (lower solid curve). The ring has $M=16$ atoms with symmetric leads ($m=n=8$). Thus at $\Phi=0$, $T=1.0$ at all 16 eigenenergies (located at each peaks, which is doubly degenerated except at the two band edges) as in the case of the resonant tunneling. T reaches a minimum value of 0.64 in between two eigenenergies. As Φ increases from zero, any doubly degenerated eigenenergy state splits into one higher and one lower energy state. Thus at $\Phi/\Phi_0=0.1$, T has peak locations moved to the new eigenergies. Now $T=0$ at eigenenergy locations of $\Phi=0$ and the peak values of T are reduced at $\Phi/\Phi_0=0.1$. The combined result appears as if a "compression" of transmission probability from any two eigenenergies of $\Phi=0$ by the magnetic flux. As Φ increases further, the compression is increased so that the two peaks, one from the higher split state of the lower quantum numbered state and one from the lower split state of the next higher quantum numbered state, are merged to form a single peak as in the case when $\Phi/\Phi_0=0.35$. As Φ increases to $\Phi/\Phi_0=0.45$, the merged peaks are reduced drastically and at $\Phi/\Phi_0=0.5$, $T=0$ at any energy. As Φ increases further from $\Phi/\Phi_0=0.5$, the trend is reversed so that at $\Phi/\Phi_0=1.0$; T reaches a complete cycle. The magnetic compression is uniform in the entire energy range because the T peaks have the same value. If the number of atoms in the ring is increased, the T peaks will be more densely packed in the same energy band.

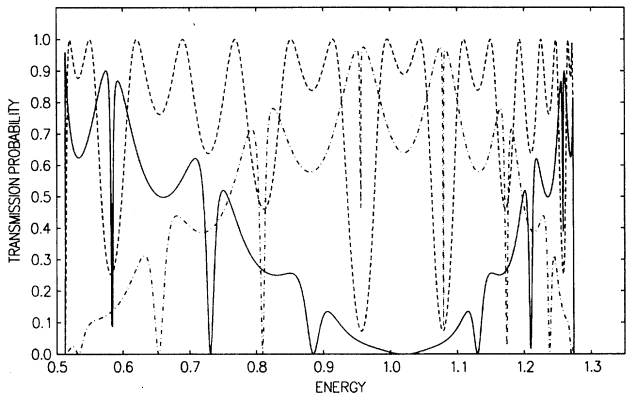

FIG. 7. Transmission probability $T(E)$ for an even-numbered metal ring with asymmetrical connecting leads. Here $M=16$ with $m=7$ is shown. The magnetic flux values are $\Phi/\Phi_0=0$ (solid curve), 0.25 (dashed curve), and 0.50 (dash-dotted curve). The "geometrical compression" on the transmission probability due to the two different electron paths along the ring is nonuniform in energy. As shown here in the case of $\Phi=0$ the reduction of the T value is much greater at the energy E near 1.02 as compared to any other location. This is due to the total cancellation of the two amplitudes from the two paths at energy $E=1.02$ (the Fermi level). As the incoming electron energy starts to deviate from that value, the degree of cancellation is reduced. This explains the "envelope" of T with respect to energy as shown by the solid curve. When magnetic flux is applied, the wavelength of propagation along the two paths will be increased (decreased) if Φ/Φ_0 is positive (negative). The degree of cancellation of amplitudes at the output node is then altered. Thus the combined geometric and magnetic compressions of T results in complicated curves obtained as shown here.

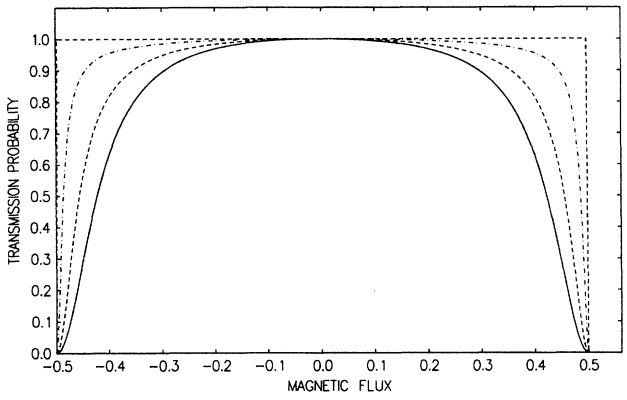

FIG. 8. Transmission probability $T(E_F)$ at Fermi energy E_F, as a function of applied magnetic flux Φ for an even-numbered mesoscopic ring of $M=36\,000$ and even-numbered paths to the two connecting leads with $m=18\,000$ (solid curve), $m=9000$ (inner dashed curve), $m=4600$ (dash-dotted curve), and $m=2$ (outer dashed curve). Single periodicity of Φ_0 is obtained for all cases. The value of T is generally close to 1.0 until Φ/Φ_0 is close to ± 0.5. However, we note that the best transmission is obtained when $m=2$.

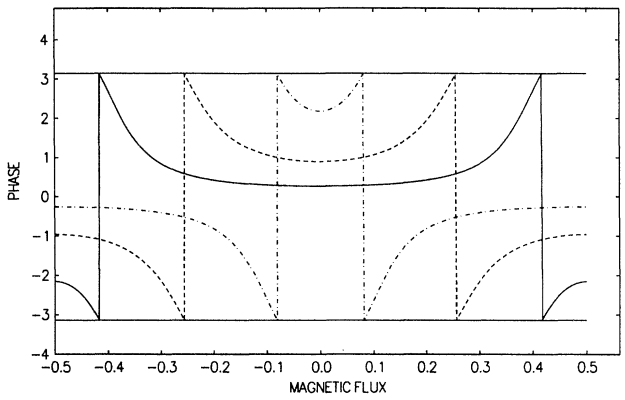

FIG. 10. Phase of the reflected wave as function of the applied magnetic flux in a one-lead ring according to Eq. (38). Here $M=17$ and $\gamma l/2=1.5$. The incoming electron energy E in units of $\hbar^2\gamma^2/\mu$ is $E=1.00$ (solid curve), 1.02 (dashed curve), and 1.04 (dash-dotted curve). Note that those energies are bounded by the two adjacent eigenenergies of $E=1.049$ and 0.927 of the ring at $\Phi=0$, which merge into $E=0.991$ at $\Phi/\Phi_0=0.5$. The sharp switch occurs whenever the incoming electron energy is in resonance with one of the eigenenergies of the ring at that particular flux [Eq. (17)].

the electron paths, composed of electrons traveling between elastic scattering centers, can be viewed as many rings of even- and odd-numbered atoms. A question then arises because the Fermi energy of each of those rings is different from all others and from the Fermi energy of the thick disordered ring. However, it can be shown that when M is large, the double periodicity remains close to the exact result of Eq. (41), even if the Fermi energy is shifted upward or downward by a small fraction of the total energy range as evaluated in Eq. (34).

V. NUMERICAL RESULTS AND DISCUSSION

We have been investigating the Aharonov-Bohm ring in terms of the underlying atomic structure. As opposed to mesoscopic descriptions, we are thus required to consider the ring and its connecting leads in terms of a discrete geometry, which can only be changed by elementary units. If there are M nodes in the ring, the leads

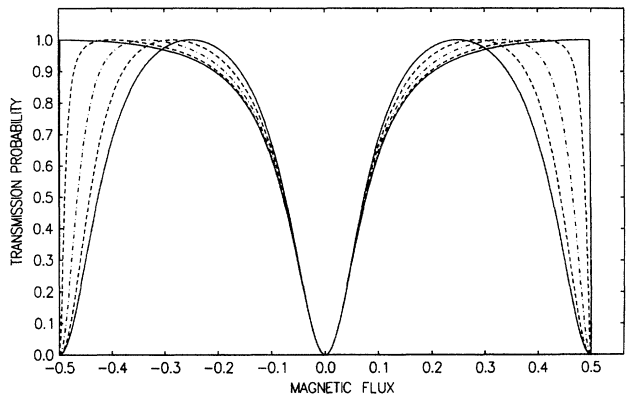

FIG. 9. Transmission probability $T(E_F)$ as a function of applied magnetic flux for an even-numbered mesoscoic ring of $M=36\,000$ as in Fig. 8 but with odd-numbered paths to the connecting leads. Here $m=17\,999$ (outer solid curve), $m=13\,501$ (outer dashed curve), $m=9001$ (dash-dotted curve), $m=4499$ (inner dashed curve), and $m=1$ (inner solid curve). Note that low transmission region is shifted to the center around $\Phi/\Phi_0=0$. Again, single periodicity is obtained in all cases. As the asymmetry value $\Delta=|m-n|$ increases, the periodicity develops a kind of double periodicity gradually. However, even at $m=1$, no exact double periodicity is achieved.

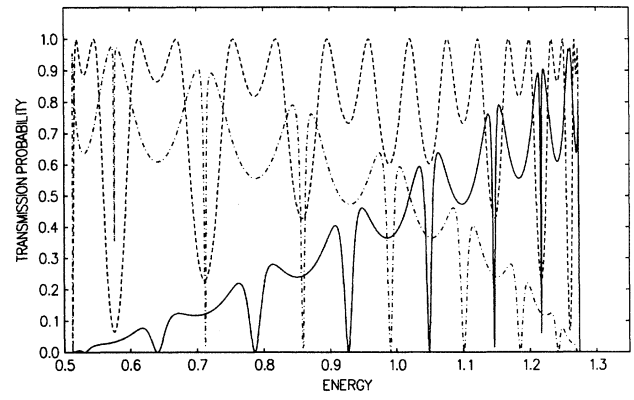

FIG. 11. Transmission probability $T(E)$ for the odd-numbered ring is shown here with $M=17$ and $m=8$. The magnetic flux is $\Phi/\Phi_0=0$ (solid curve), 0.25 (dashed curve), and 0.50 (dash-dotted curve). The results indicate the presence of both geometrical and magnetic compressions.

define a partition $m+n=M$. $\Delta=|m-n|$ described the deviation from symmetry.

A. M even, $\Delta=0$

For an exact symmetric ring, our results agree with Ref. 11 and the transmission probability $T(E)$ as a function of energy exhibits a peak transmission ($T=1.0$) whenever the incident electron energy coincides with one of the eigenenergies of the ring and reaches a minimum value of $T=0.64$, reflecting the coupling strength of the leads, in between when there is no magnetic flux present (Fig. 6, upper solid curve). As the magnetic flux is turned on, T jumps to zero at all the eigenenergies for $\Phi=0$ and the transmission probability in between any two eigenenergies of $\Phi=0$ is compressed from the two zeros. This compression arises from the splittings of the doubly degenerated eigenenergies of $\Phi=0$ and the reduction of the T value when the magnetic flux is applied. T now exhibits peaks at the new eigenenergies, which are shifted towards the middle between any adjacent two eigenenergies of the $\Phi=0$ case. As Φ increases further, those two peaks are merged into one and the peak value starts to drop until $\Phi/\Phi_0=0.5$. At that value, $T=0$ for all incoming waves. This is shown in Fig. 6. As Φ increases further, the behavior of T is reversed so that at $\Phi/\Phi_0=1.0$, T completes a period. We note that the "magnetic compression" of the transmission probability is uniform over the entire energy range for a symmetric ring, because of the product form of the numerator in Eq. (36). For different values of $\gamma l/2$, the behavior of T is similar, except it is distributed over different bandwidths. Thus, for a free-electron network, $T(E)$ is distributed over an infinite energy range, while for a tight-binding network, $T(E)$ is simply "squeezed" into a narrow energy range with the same behavior as the case of free-electron network. In our calculations of $T(E)$, we have delibrately chosen small values of M for clarity of the figures presented. If M is increased, the oscillatory behavior in between two eigenenergies is similar to what we have presented here but the total number of oscillatory segments is increased in the same energy bandwidth.

B. M even, $\Delta\neq 0$

If M is an even number and m deviates from the perfect symmetry (given by $m=M/2$), however, $T=0$ at all eigenenergies when $\Phi=0$. The degree of compression on the transmission probability is different in different energy ranges. This is shown in Fig. 7. The "geometric compression" is now due to the different degree of cancellation of the two amplitudes, coming from the two paths joining at the output node, from different input electron energy, or different wavelength.

C. $T(E_F)$ for M even, Δ even

The transmission probability at E_F for $M=36\,000$ atoms ($r_0\sim 1$ μm) for exact symmetry and for $\Delta=$even is shown in Fig. 8 as a function of the magnetic flux. In those cases, the best transmission is obtained except when Φ/Φ_0 is near ± 0.5.

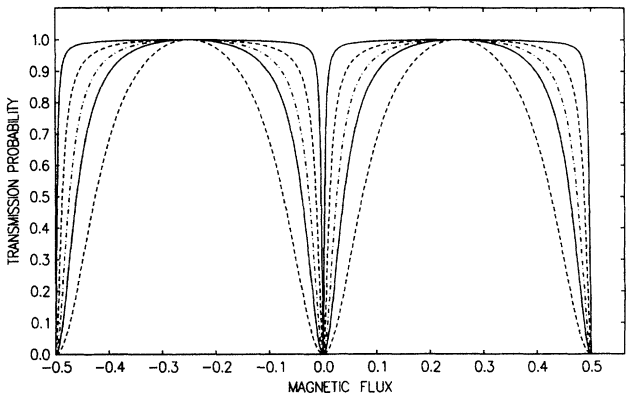

FIG. 12. Transmission probability $T(E_F)$ for an odd-numbered mesoscopic ring of $M=36\,001$. The configuration closest to a symmetric ring is when $m=18\,000$ (inner solid curve). A mathematically exact double periodicity is obtained for any $\Delta=|m-n|$. Shown here is $m=13\,500$ (dash-dotted curve), $m=9000$ (outer dashed curve), $m=4500$ (outer solid curve), and $m=1$ (inner dashed curve). (See Sec. IV for proof of universal double periodicity.)

D. $T(E_F)$ for M even, Δ odd

In Fig. 9 we show the corresponding cases when Δ is odd. For small Δ, the low transmission region is around $\Phi=0$. However, as Δ increases, the transmission gradually develops a kind of double periodicity, although even at $\Delta=35\,998$, the $\Phi_0/2$ periodicity is not mathematically exact.

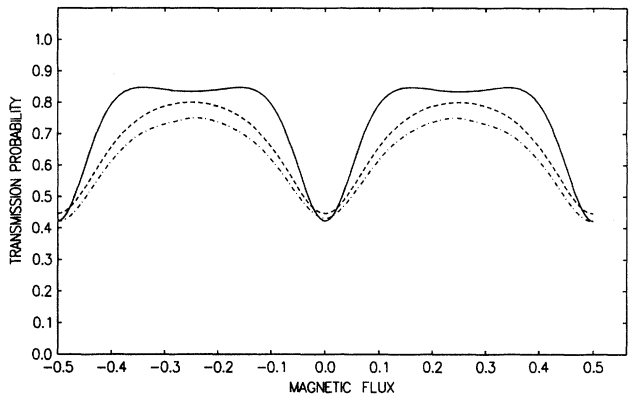

FIG. 13. Transmission probability $\langle T\rangle$ at finite temperature T_0 for an odd-numbered ring. Here an $M=361$ and $m=180$ ring is calculated for a metallic model using the form factor given by Eq. (16) at $\gamma l/2=1.5$. The dimensionless bandwidth $E_g(\mu/\hbar^2\gamma^2)$ is 0.76 so that the average spacing between two eigenenergies is $\Delta E=E_g(\mu/\hbar^2\gamma^2 M)=0.0021$. The values of $kT_0(\mu/\hbar^2\gamma^2)$ are 0.0005 (solid curve), 0.002 (dashed curve), and 0.076 (dash-dotted curve). Thus double periodicity for odd-numbered ring survives the temperature averaging. Similarly, single periodicity of even-numbered and symmetric rings remains the same after the same temperature averaging.

E. One-lead metal ring

In Fig. 10, we show the phase of a reflected wave from the extreme one-lead ring according to Eq. (38). Whenever the incoming electron energy from the lead is equal to one of the eigenenergies of the ring, the reflected wave will accumulate an integer phase factor of 2π. Thus, if the incoming electron energy is steadily increased from one eigenenergy to the next higher one, while keeping the magnetic flux constant, the phase of the reflected wave will decrease by a factor of 2π during that period. Thus, one can consider the one-lead crystal rings as a "phase valve," where the phase of the reflected wave can be "tuned" by the threaded magnetic flux. Here we show that for a given incoming electron energy, the phase of the reflected wave gradually increases with the applied magnetic flux and then sharply decreases by a factor of 2π when that incoming energy becomes in resonance with one of the eigenenergies of the ring. Such sharp phase switching is not guaranteed in the disordered ring because the electron energy may lie in the band gaps of the metallic ring.

F. *M* odd

For an odd-numbered ring, it is not possible to have exact symmetrical lead positions. The configuration closest to a symmetric ring is when $\Delta=|m-n|=1$. Thus the incoming electron wave incident on the $j=m+1$ node will travel on two paths differing by at least one atomic spacing: Δ is odd for any m. In the case of $\Delta=1$, the transmission probability is zero at the eigenenergies of the ring when $\Phi=0$. The behavior of $T(E,\Phi)$ as a function of E and Φ is shown in Fig. 11. The combined geometric and magnetic compressions on $T(E)$ is evident as in Fig. 7. Double periodicity as derived in Sec. IV is shown in Fig. 12 for $M=36\,001$. This is to be compared with the single periodicity for $M=36\,000$ as shown in Fig. 8.

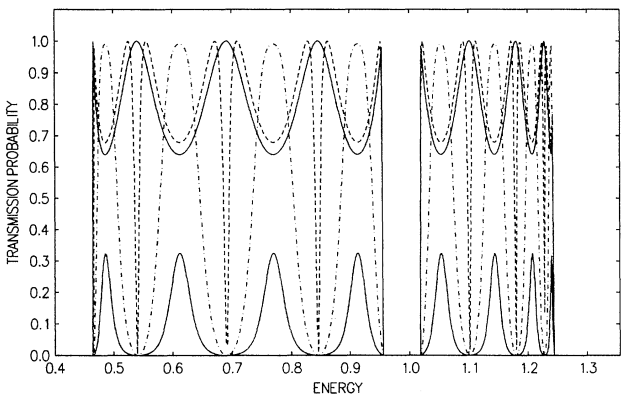

FIG. 14. Transmission probability $T(E)$ as a function of incoming electron energy, for a semiconductor ring, using the form factor derived in Eq. (26). Here $M=16$ and $\gamma_0 l_0/2=1.5$ and $\gamma_1 l_1/2=1.45$ are used for a symmetric ring. The magnetic flux is $\Phi/\Phi_0=0$ (upper solid curve), $\Phi/\Phi_0=0.1$ (dashed curve), $\Phi/\Phi_0=0.35$ (dash-dotted curve), and $\Phi/\Phi_0=0.45$ (lower solid curve). The energy E is in units of $\mu/\hbar^2\gamma_0$ and $l_0=l_1=l/2$. The result is similar to that of a metal ring as illustrated in Fig. 6 except that there exists an energy gap as described in the text.

G. Finite temperature

At finite temperature, the transmission probability is averaged over a small energy range so that[12]

$$\langle T\rangle=\int T(E)\frac{df}{dE}dE\ , \tag{46}$$

where f is the Fermi distribution. Equation (46) is calculated and shown in Fig. 13 for various values of temperature for an odd-numbered ring. We show that the double periodicity can survive the temperature averaging. Similarly, $\langle T\rangle$ for an even-numbered ring survives the temperature averaging and remains at the single periodicity.

H. Semiconductor ring

Finally, the transmission probability in a semiconductor ring can also be evaluated using the form factor derived in Eq. (26). The behavior of T is similar to that of a metallic ring except that the energy range is split into two regions separated by a gap as one would expect from a semiconductor material. This is shown in Fig. 14.

VI. CONCLUSIONS

We have formulated an exactly solvable quantum-network theory of transport by properly relating the reflection coefficient with the phase factor of the wave function associated with the 1D path between two nodes. The node equation approach, derived from the use of Kirchhoff's law, has been shown to be convenient for calculating the transmission probability and is useful for evaluating complicated networks. The use of form factors allows one to model metallic as well as semiconductor networks and even realistic materials, provided such a factor can be obtained. Thus the network theory is based on an explicit structure model.

The exact transmission probability for generalized Aharonov-Bohm ring is obtained for a clean crystal. The Green's-function approach shown in the derivation allows one to generalize to include some disorder in the ring as well as different types of connecting materials. The even- and odd-numbered rings have a distinctly different transmission behavior. The double periodicity in the odd-numbered ring is exact. It is a universal double periodicity regardless of the two connecting locations and the form factor used. So long as crystallinity is maintained in the sample, this double periodicity will prevail from mesoscopic scale to molecular scale. The origin of periodicity is the standing wave produced by a crystalline ring and that this double periodicity survives the temperature averaging. The fact that electrons travel on two large paths differing by just one atomic spacing before joining together can result in totally different behavior in quantum transport.

ACKNOWLEDGMENTS

One of us (C.H.W.) acknowledges financial support from Max-Planck Institute for Solid State Research at Stuttgart, Federal Republic of Germany. He also would like to thank T. Held and K. Scheller for computing assistance.

*Permanent address.
[1]L. Pauling, J. Chem. Phys. **4**, 673 (1936).
[2]C. Coulson, Proc. Phys. Soc. (London) **67**, 608 (1954).
[3]K. Rudenberg and C. Scherr, J. Chem. Phys. **21**, 1965 (1953).
[4]G. Della Riccia, *Proceedings of the International Conference on Semiconductors, Exeter, 1962* (The Institute of Physics and the Physical Society, London, 1962), p. 570.
[5]M. Weger, S. Alexander, and G. Della Riccia, J. Math. Phys. **14**, 259 (1973).
[6]E. Montroll, J. Math. Phys. **11**, 635 (1970).
[7]E. Montroll, J. Phys. Chem. Solids **34**, 597 (1973).
[8]C. H. Wu and E. Montroll, J. Nonmet. Semicond. **2**, 153 (1975).
[9]C. H. Wu and F. T. Lee, J. Phys. Chem. Solids **46**, 1255 (1985).
[10]M. Buttiker, Y. Imry, and R. Landauer, Phys. Lett. **96A**, 365 (1983).
[11]M. Buttiker, Y. Imry, and M. Azbel, Phys. Rev. A **30**, 1982 (1984).
[12]M. Buttiker, Y. Imry, R. Landauer, and S. Pinhas, Phys. Rev. B **31**, 6207 (1985).
[13]R. Webb, S. Washburn, C. Umbach, and R. Laibowitz, Phys. Rev. Lett. **54**, 2696 (1985).
[14]C. Umbach, C. Van Haesendonck, R. Laibowitz, S. Washburn, and R. Webb, Phys. Rev. Lett. **56**, 386 (1986).
[15]S. Datta, M. Melloch, S. Bandyopadhyaay, R. Noren, M. Vaziri, M. Miller, and R. Reifenberger, Phys. Rev. Lett. **55**, 2344 (1985).
[16]R. Webb and S. Washburn, Phys. Today **41** (12), 46 (1988).
[17]Y. Gefen, Y. Imry, and M. Azbel, Phys. Rev. Lett. **52**, 129 (1984).
[18]A. Stone and Y. Imry, Phys. Rev. Lett. **56**, 189 (1986).
[19]A. Aronov and Y. Shavin, Rev. Mod. Phys. **59**, 755 (1987).
[20]S. Datta, Superlatt. Microstructures **6**, 83 (1989).
[21]M. Heiblum, M. Nathan, D. Thomas, and C. Knoedler, Phys. Rev. Lett. **55**, 2200 (1985).
[22]A. Staring, L. Molenkamp, C. Beenakker, L. Kouwenhoven, and C. Foxon, Phys. Rev. B **12**, 8461 (1990).
[23]R. Landauer, Philos. Mag. **21**, 863 (1970).
[24]R. Landauer and M. Buttiker, Phys. Rev. Lett. **54**, 2049 (1985).
[25]B. Doucot and R. Rammal, Phys. Rev. Lett. **55**, 1148 (1985).
[26]P. de Gennes, C. R. Acad. Sci. B **292**, 279 (1981).
[27]S. Alexander, Phys. Rev. B **27**, 1541 (1983).
[28]J. Avron, A. Raveh, and B. Zur, Rev. Mod. Phys. **60**, 873 (1988).
[29]J. Ziman, *Principles of the Theory of Solids* (Cambridge University Press, Cambridge, 1965), Chap. 3.
[30]R. Mills and E. Montroll, J. Math. Phys. **11**, 2525 (1970).
[31]N. Trivedi and D. Browne, Phys. Rev. B **38**, 9581 (1988).
[32]V. Ambegaokar and U. Eckern (unpublished).
[33]B. Al'tshuler, A. Aronov, and B. Spivak, Pis'ma Zh. Eksp. Teor. Fiz. **33**, 101 (1981) [JETP Lett. **33**, 94 (1981)].